

Precise frequency estimation in a microelectromechanical parametric resonator

Michael V. Requa^{a)} and Kimberly L. Turner

Department of Mechanical and Environmental Engineering, University of California at Santa Barbara, Santa Barbara, California 93106

(Received 20 February 2007; accepted 25 March 2007; published online 25 April 2007)

The authors report here on precise resonant frequency estimation using the nonlinear spectral features of parametric resonance. Demonstration of 100 parts per 10^9 frequency resolution at room temperature is accompanied by a technique to observe the phase trajectories of escape in bistable parametrically resonant systems. The system offers an expanded dynamic range over similar linear resonators. Precise frequency estimation has implications in resonant mass sensing. © 2007 American Institute of Physics. [DOI: 10.1063/1.2732172]

Resonant mass and force sensing have made recent strides, demonstrating zeptogram scale mass sensitivity¹ and single electron spin mechanical force measurement.² Recent studies report that the dynamic range of a resonator has a critical influence on mass sensitivity sensors.³ Harmonic resonance based detection is the established convention for resonant physical sensors. Linear harmonic sensors are limited, on the upper bound, by mechanical nonlinearities.⁴ Although sensors that use nonlinear features can be described by the same governing equation as those that use linear features, the sensing mechanism is drastically different in nature. The so-called Duffing oscillator model is widely used to describe nano- and microscale resonators. This work examines a close relative to this system, a parametrically resonant transducer in the interest of determining its potential as a resonant mass sensor. It has been postulated that nonlinear spectral features may enhance sensitivity,^{5,6} if for no other reason than because using these features allows for greater dynamic range. The discontinuity in the nonlinear spectrum may also be a superior noise rejection mechanism.

The parametric resonator under examination here can be described by the following differential equation:

$$\ddot{q} + \mu\dot{q} + \omega_0^2 q + \gamma q^3 + \lambda q \cos \omega t = \xi(t), \quad (1)$$

where $\xi(t)$ represents a stochastic forcing term which will be ignored in the analysis but ultimately limits the precision of such measurements. Insight can be gained by examining the slow varying envelope of the system. This analysis is carried out by using an averaging equation by introducing slow varying quadrature averages (q_1, q_2) ,⁷

$$q = q_1 \cos \frac{\omega t}{2} - q_2 \sin \frac{\omega t}{2},$$

$$\frac{dq}{dt} = -\frac{\omega}{2} \left(q_1 \sin \frac{\omega t}{2} + q_2 \cos \frac{\omega t}{2} \right). \quad (2)$$

Substituting Eq. (2) into Eq. (1) and averaging, we get a system for the “slow” variables,

$$\dot{q}_1 = -\mu q_1 + 2\Omega q_2 + \frac{\lambda}{\omega} q_2 - \frac{3\gamma}{2\omega} q_2 (q_1^2 + q_2^2),$$

$$\dot{q}_2 = -\mu q_2 - 2\Omega q_1 + \frac{\lambda}{\omega} q_1 + \frac{3\gamma}{2\omega} q_1 (q_1^2 + q_2^2), \quad (3)$$

where $\Omega = \omega/2 - \omega_0$, which is defined as the detuning of the system. By linearizing Eq. (3) in the limit of small amplitude, it can be seen that for certain driving parameters, $\lambda > \omega_0^2/4Q$ and $\Omega \sim 0$, there exist positive real eigenvalues resulting in linear instability of the system. The instability causes growth in the oscillation amplitude limited by the nonlinear term with coefficient γ . Parametric resonance, synonymous here with linear instability, has two stable fixed points of equal magnitude but separated in phase by π rad.⁸

The symmetric fixed points are apparent in numerical simulations of the phase space of Eq. (3) presented in Fig. 1. Parametric resonance with a cubic nonlinearity has three distinct solution regions which are segregated by two pitchfork bifurcation points, $\Omega_B = \pm \sqrt{(\lambda/4\omega_0)^2 - (\mu/2)^2}$. The region where $\Omega > \Omega_B$ in this case is nonresonant and has only a trivial zero amplitude solution. Resonance, where $-\Omega_B < \Omega < \Omega_B$, has two symmetric stable fixed points about the unstable fixed point at the origin. The third region, where

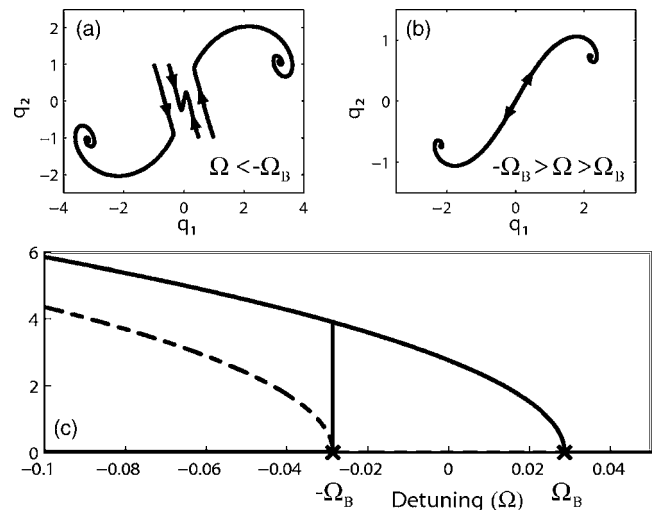


FIG. 1. Simulated response of the “slow” variable system. (a) Nonresonant phase space below critical detuning $-\Omega_B$ shows three stable fixed points and corresponding attractors. Origin in this region is stable. (b) Phase space for resonant region; origin here is unstable. (c) Simulated spectrum for parametric resonance; bifurcation which changes the stability of the origin causes large jump in amplitude.

^{a)}Electronic mail: requa@enr.ucsb.edu

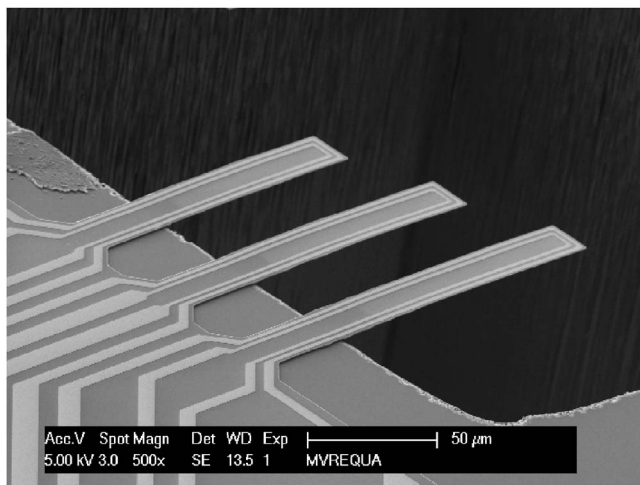


FIG. 2. Scanning electron microscopy of devices used in the experiment. Two metal lines allow for the segregation of drive and sense channels.

$\Omega < -\Omega_B$, has three stable fixed points including two symmetric large amplitudes and the origin, forming three stable attractors. This description is accurate for systems with negative nonlinear coefficients, $\gamma < 0$. Systems with positive nonlinear coefficients demonstrate the same features but are reversed in relationship to detuning, Ω . Simulating the spectral response of the amplitude we see that the bifurcation introduces dramatic spectral features. At driving frequencies below the critical frequency $\Omega < -\Omega_B$ there exists a zero amplitude attractor. Crossing the subcritical bifurcation makes this fixed point unstable. If a resonator is prepared in the zero amplitude stable state and the system is tuned across the bifurcation, the resonator will jump to a high amplitude solution. The frequency of the bifurcation jump, by this technique, is a biased estimator of the resonant frequency and the proposed sensing mechanism.

We report here on measurements performed using a cantilever transducer which is driven and sensed electrically. The transducer physics was reported earlier, with only subtle differences.⁹ In this case, the cantilever is a continuous material and there are two conducting paths, one for the drive signal and the other for sense signal (Fig. 2). The silicon cantilever used in this study has dimensions of 200 nm thick, 20 μm wide, and 80 μm long with a resonant frequency near 29.6 kHz and quality factor of approximately 4000. The quality factor was characterized by driving the device with a bulk piezoelectric crystal, measuring the oscillations with a laser vibrometer, and fitting the acquired harmonic resonant curve by a least-squares fit routine.

Amplitude demodulation of the oscillation signal for parametrically resonant transducers is nontrivial because the driving signal and sensing signal are at $2\times$ frequency multiples. For these measurements we employ two function generators using the same clock signal but generating signals at ω and 2ω , respectively (Fig. 3). Using a reference signal at ω and a lock-in amplifier enables not only measurements of the nonlinear spectrum but also of the phase space trajectories of the “jump” phenomenon. Experiments were run at room temperature and inside of a vacuum chamber at pressures near 10^{-4} Torr. To identify the bifurcation point, continuous sweeps in frequency were performed for various drive strengths mapping the amplitude dependent spectra (Fig. 4). The data demonstrate the expected jumps in amplitude cor-

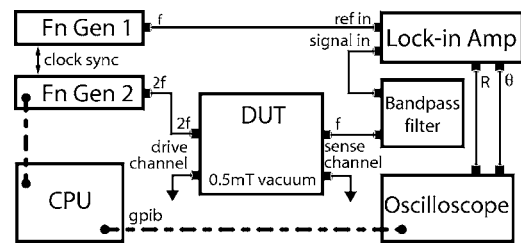


FIG. 3. Instrumentation used in experiments allows measurement of “slow” variable envelope by generating a synchronous reference signal to demodulate the sensing signal which is at half the frequency of the drive.

responding to the bifurcation points. Trajectories of the escape events were also recorded. The data show two symmetric fixed points of equivalent amplitude but separated by π rad, which is in agreement with simulation. A spurious mode can be seen in the data for all traces near 29.6 kHz, one possible cause of this is stochastic telegraph signals between attractors for small amplitudes where the barrier to escape is near zero.

It is the amplitude jump that constitutes the frequency estimator in the proposed application. The essence of the experiment is to prepare the system in the low amplitude attractor sufficiently far, in frequency, from the bifurcation such that transitions are statistically unlikely. Then incrementally increase the drive frequency at a controlled rate to approach the bifurcation until the system jumps to a high amplitude solution, at which point the drive frequency is recorded. In a deterministic system, this jump would occur at the exact point of stability change ($-\Omega_B$) with limitless resolution. The noisy nature of a real system [$\xi(t) \neq 0$] dictates that escape will occur at a frequency of some uncertainty.⁷ This process is repeated a large number of times to get a statistically significant data set. The variance of the jump events from the median jump frequency will give a measure of the precision of this measurement technique.

An experiment as described above was performed with a driving strength of 3.0 mA, corresponding to the bold line

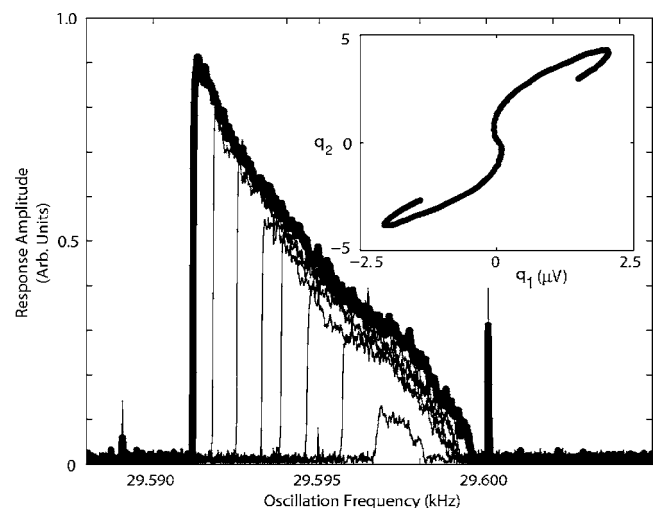


FIG. 4. Observations of parametric resonance in experimental device. Spectra show asymmetry of resonance for different driving amplitudes between 2.3 and 3.0 mA, with 0.1 mA step size, increasing response corresponds to increasing driving signal. Bold line is spectral data using 3.0 mA drive signal. (Inset) Experimental data of escape trajectories on a 3.0 mA spectral line. Experiment demonstrates symmetric escape paths from the zero amplitude fixed point.

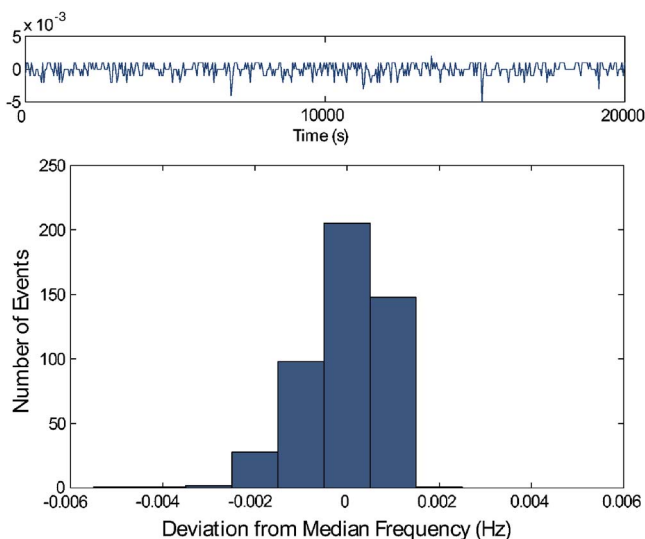


FIG. 5. Top plot is the frequency of the amplitude jump relative to the median with respect to time. Bottom is histogram of time series data. 98% of events occur within ± 0.002 Hz of the median.

spectrum and the displayed escape trajectories shown in Fig. 4. Frequency was swept at a rate of 0.6 Hz/min (or step size of 0.001 Hz and hold time of 0.1 s) at a starting frequency of 29 586.2 Hz. The jump transition was observed 500 times over the span of several hours. To achieve the long term frequency stability the sample was kept in a vacuum for several days after several nitrogen and vacuum purge cycles. The results of the experiment are presented in Fig. 5. The experiment shows a frequency resolution precise to ± 0.002 Hz with a median of 29 586.453 Hz. This corresponds to a frequency resolution of $d\omega_0/\omega_0 \sim 10^{-7}$ at room temperature. The analytical results of a previous study³ consider mass resolution to be a product of resonator mass and fractional frequency resolution ($dM_0 = 2M_{\text{res}}d\omega_0/\omega_0$). By this argument and using the approximate mass of the cantilever

(1 ng), the demonstrated frequency resolution is 200 ag. Recent studies have shown transduction in nanometer scale cantilevers.¹⁰ Further miniaturization to these standards would mean inertial benefits in the sensitivity of three orders. In a previous work, we demonstrated that these dynamics can be observed in resonators using a single conductor,⁹ which may enable miniaturization.

We introduce here a technique for observing the phase trajectories of a parametric resonance in a microelectromechanical system oscillator. The matching features of the experimentally measured phase trajectories (Fig. 4) and the numerically simulated (Fig. 1) are strong indicators of the accuracy of the model. We also report on a study of frequency resolution by the measurement of nonlinear spectral features. The fractional frequency resolution of $d\omega_0/\omega_0 \sim 10^{-7}$ reported here at room temperature rivals other recent demonstrations of precision resonant frequency measurement in nanoscale resonators at supercooled temperatures by both linear¹⁰ and nonlinear⁶ techniques.

The authors would like to acknowledge Mark Dykman and Andrew Cleland for many useful discussions.

- ¹Y. T. Yang, C. Callegari, X. L. Feng, K. L. Ekinci, and M. L. Roukes, *Nano Lett.* **6**, 583 (2006).
- ²D. Rugar, R. Budakian, H. J. Mamin, and B. W. Chui, *Nature (London)* **430**, 329 (2004).
- ³K. L. Ekinci, X. M. H. Huang, and M. L. Roukes, *Appl. Phys. Lett.* **84**, 4469 (2004).
- ⁴B. Yurke, D. S. Greywall, A. N. Pargellis, and P. A. Busch, *Phys. Rev. A* **51**, 4211 (1995).
- ⁵K. L. Turner, S. A. Miller, P. Hartwell, N. C. MacDonald, S. H. Strogatz, and S. G. Adams, *Nature (London)* **396**, 149 (1998).
- ⁶J. S. Aldridge and A. N. Cleland, *Phys. Rev. Lett.* **94**, 156403 (2005).
- ⁷M. I. Dykman, C. M. Maloney, V. N. Smelyanskiy, and M. Silverstein, *Phys. Rev. E* **57**, 5202 (1998).
- ⁸A. H. Nayfeh and D. T. Mook, *Nonlinear Oscillations* (Wiley-Interscience, New York, 1977), p. 258.
- ⁹M. V. Requa and K. L. Turner, *Appl. Phys. Lett.* **88**, 263508 (2006).
- ¹⁰M. Li, H. X. Tang, and M. L. Roukes, *Nature Nanotech.* **2**, 114 (2007).